

TURBINE BLADE CRACK DETECTION USING VIBRATION TESTING  
METHODS

GUAI YEU KAE

UNIVERSITI TEKNOLOGI MALAYSIA

TURBINE BLADE CRACK DETECTION USING VIBRATION TESTING  
METHODS

GUAI YEU KAE

A thesis submitted in fulfilment of the  
requirements for the award of the degree of  
Master of Engineering (Mechanical)

Faculty of Mechanical Engineering  
Universiti Teknologi Malaysia

DEC 2009

To Papa, Mama and Tan Lin  
for their support and love

## ACKNOWLEDGEMENT

I would like to express my sincere appreciation and gratitude to my thesis supervisor, Prof. Ir. Dr. Mohd. Salman Leong, for his supervision, helpful encouragement, knowledge, continued guidance and moral support throughout my studies as well as freedom provided to work on this research. I am also grateful to my colleagues, Wong, Tan and Asrie, for sharing their ideas and providing valuable suggestions; laboratory assistants, Ali, for his patience, for answering endless questions and making the time spent together working at the IKG laboratory a valuable experience for me; Many thanks are also due to the staff of IKG, Kak Ana, for her support and assistance in my studies.

Special thanks to Lim Chai Heng and Goh Hui Minn. Their great dedication towards assisting me was above and beyond what I expected. I truly appreciated their true friendship.

I would like to thank Papa, Mama, my sister and Tan Lin for their unswerving belief and support to me all these years.

## ABSTRACT

Turbine blades are the most common cause of failures in gas turbines. Failure modes are typically cracking from foreign object damage (FOD), high cycle stress (HCF), blade rubbing, degradation from erosion and corrosion. Fault detection of blades is important function in reducing blade related failures. This study involved the use of vibration analysis and dynamic testing of blades for failure detection. Current field inspections of blades are based on visual inspections only, and the intent here was to use impact testing of the blades during these inspections to determine cracked blade (from the vibration response). Vibration impact tests were undertaken using decommissioned turbine blades with and without cracks in the laboratory. Four common crack patterns were deliberately induced to the turbine blades to investigate changes in the blades normal mode response. Finite element analysis (FEA) of the blades was also undertaken. FEA results were correlated to experimental results and these results showed that each crack pattern was unique and significant changes were found in higher modes. Dynamic vibration analysis was also undertaken in a laboratory testrig fitted with rotating model straight blades. Vibration measurements were undertaken on a baseline test case and other test conditions where the blades had induced cracks. Steady state and transient vibration responses were obtained from the controlled tests. Vibration measurements were on the machine casing and on a blade (with an accelerometer surfaced mounted onto a rotating blade). Order tracking analysis and continuous wavelet analysis were performed to the measured data. Both techniques showed ability in detecting changes in vibration response on the blades and casing for blades with cracks. Results showed that significant changes were detected during transient analysis as compared to the steady state. Changes were noted in the vibration response corresponding to the machine running speed and blade passing frequencies. Changes in wavelet maps were however qualitative in nature, which suggested that more work need to be undertaken for cracks severity assessment using wavelet maps.

## ABSTRAK

Bilah turbin adalah salah satu punca utama yang menyebabkan kegagalan dalam turbin-turbin gas. Kegagalan biasanya terjadi disebabkan oleh kerosakan objek asing (FOD), tekanan kitaran tinggi (HCF), geseran bilah dan degradasi daripada hakisan dan kakisan. Kajian ini melibatkan penggunaan analisis getaran dan ujian dinamik bilah turbin untuk mengesan kegagalan bilah. Tujuan kajian ini adalah dengan menggunakan ujian impak bilah bagi menentukan kegagalan bilah (daripada tindakbalas getaran). Ujian impak getaran ini telah dijalankan dengan menggunakan bilah turbin yang mempunyai dan tidak mempunyai retakan. Empat jenis corak retak telah dikenakan pada bilah turbin bagi mengkaji perubahan pada bilah turbin itu ketika dalam mod yang biasa. Analisis unsur terhingga bilah turbin juga dijalankan. Keputusan analisis unsur terhingga telah dikorelasikan dengan hasil keputusan kajian. Keputusan ini menunjukkan bahawa perubahan setiap corak retakan adalah unik dan penemuan ketara telah ditemui dalam mod yang lebih tinggi. Analisis getaran dinamik telah dijalankan di alatan ujian yang dipasang dengan bilah turbin lurus yang berputar. Getaran mantap dan getaran fana diperolehi dari ujian yang dikawal itu. Pengukuran getaran dilakukan pada penutup mesin dan pada salah satu bilah (dengan satu meter pecutan yang dilekatkan pada bilah yang berputar). Analisis pengesanan arah (order tracking) dan analisis gelombang kecil (wavelet analysis) selanjut dilakukan pada data yang diperolehi. Kedua-dua teknik ini menunjukkan keupayaan dalam mengesan perubahan tindakbalas getaran. Keputusan menunjukkan perubahan yang ketara telah dikesan semasa analisis fana berbanding pada keadaan mantap. Perubahan telah dikenalpasti di dalam tindakbalas getaran berdasarkan kepada halaju mesin dan frekuensi halaju bilah. Perubahan dalam peta gelombang kecil bagaimanapun adalah secara semulajadi dan dicadangkan bahawa kajian yang lebih mendalam perlu dilakukan bagi mengesan retakan yang teruk dengan menggunakan peta gelombang kecil.

## TABLE OF CONTENTS

CHAPTER	TITLE	PAGE
	DECLARATION	ii
	DEDICATION	iii
	ACKNOWLEDGEMENT	iv
	ABSTRACT	v
	ABSTRAK	vi
	TABLE OF CONTENTS	vii
	LIST OF TABLES	xi
	LIST OF FIGURES	xiii
	LIST OF ABBREVIATIONS	xxi
	LIST OF APPENDICES	xxii
<b>1</b>	<b>INTRODUCTION</b>	<b>1</b>
	1.1 Overview	1
	1.2 Subject Background	4
	1.3 Problem Statement	6
	1.4 Objectives of the Study	7
	1.5 Scopes of the Study	7

<b>2</b>	<b>LITERATURE REVIEW</b>	<b>8</b>
2.1	Introduction	8
2.2	Static Test Condition	9
2.3	Dynamic Test Condition	10
2.3.1	Wavelet Analysis	10
2.3.2	Order Tacking	11
2.3.3	Other Analysis Method	11
<b>3</b>	<b>OVERVIEW OF VIBRATION ANALYSIS</b>	<b>12</b>
3.1	Introduction	12
3.2	Fast Fourier Transform	13
3.3	Wavelet Analysis	14
<b>4</b>	<b>RESEARCH METHODOLOGY</b>	<b>16</b>
4.1	Overview	16
4.2	Stationary Test Condition	19
4.3	FEA Modeling	19
4.4	Dynamic Test Condition	20
<b>5</b>	<b>EXPERIMENTAL SET UP AND PROCEDURE</b>	
	<b>PART I: STATIONARY TEST METHODS</b>	<b>21</b>
5.1	Introduction	21
5.2	Test Rig Assembly	22
5.3	Instrumentation and Calibration	24
5.4	Experimental Procedures	28
<b>6</b>	<b>COMPUTATIONAL STUDY USING FINITE ELEMENT ANALYSIS</b>	<b>32</b>
6.1	Introduction	32



6.2	Preprocessing	33
6.3	Model Analysis	36
6.4	Post Processing	37
<b>7</b>	<b>EXPERIMENTAL SET UP AND PROCEDURE</b>	
	<b>PART II: DYNAMIC TEST METHODS</b>	38
7.1	Introduction	38
7.2	Experimental Rig Assembly	39
7.3	Instrumentation and Calibration	40
7.4	Experimental Procedures	42
<b>8</b>	<b>EXPERIMENTAL RESULTS AND DISCUSSION</b>	43
8.1	Overview	43
8.2	Experimental Results: Part I	
	Stationary Test Conditions	44
	8.2.1 Cracks on The Air-Flow Leading Edge	49
	8.2.2 Cracks on The Air-Flow Trailing Edge	53
	8.2.3 Blade Root Cracks	56
	8.2.4 Foreign Object Damage (FOD) at Blade Tip	59
8.3	Computational Study	62
	8.3.1 Air-Flow Lead Crack	64
	8.3.2 Air-Flow Trail Crack	66
	8.3.3 Blade Root Crack	68
	8.3.4 Foreign Object Damage (FOD) at Blade Tip	70
8.4	Experimental Results: Part II	
	Dynamic Test Conditions	72
	8.4.1 Transient Analysis	76
	8.4.1.1 Air-Flow Lead Crack	77
	8.4.1.2 Air-Flow Trail Crack	93
	8.4.1.3 Blade Root Crack	100
	8.4.1.4 Foreign Object Damage (FOD) at Blade Tip	108

8.4.1	Steady State Conditions	116
8.4.2.1	Air-Flow Lead Crack	118
8.4.2.2	Air-Flow Trail Crack	124
8.4.2.3	Blade Root Crack	127
8.4.2.4	Foreign Object Damage (FOD) at Blade Tip	129
<b>9</b>	<b>CONSOLIDATED FINDINGS AND DISCUSSION</b>	<b>130</b>
9.1	Overview	130
9.2	Stationary Test Conditions & FEA Modeling	130
9.3	Dynamic Test Conditions	140
<b>10</b>	<b>CONCLUSIONS AND RECOMMENDATIONS</b>	<b>145</b>
10.1	Overview	145
10.2	Conclusion for Static Test Method and Computational FEA Study	146
10.3	Conclusion for Dynamic Test Method	146
10.4	Recommendations for Future Work	147
	<b>REFERENCES</b>	<b>149</b>
	Appendices A1-A4	153-180

## LIST OF TABLES

TABLE NO.	TITLE	PAGE
5.1	Tabulation of instruments	27
7.1	Tabulation of instruments	42
8.1	Blade's (airflow lead crack) natural frequencies under various cracks length.	50
8.2	Blade's (airflow trail crack) natural frequencies under various crack length.	54
8.3	Blade's (root crack) natural frequencies under various cracks length	57
8.4	Blade's (FOD) natural frequencies under various cracks length.	60
8.5	FEA Results of model blade with air-flow lead crack under different percentage of crack	64
8.6	FEA Results of model blade with air-flow trail crack under different percentage of crack	66
8.7	FEA Results of model blade with blade root crack under different percentage of crack	68
8.7	FEA Results of model blade with FOD at blade tip under different percentage of crack	70
8.9	Comparison of order tracking results (0% crack to 75% crack) on blade vibration under air-flow lead crack scenario.	81
8.10	Comparison of order tracking results (0% crack to 75% crack) on axial casing vibration under air-flow lead crack scenario	87

8.11	Comparison of order tracking results (0% crack to 75% crack) on horizontal casing vibration under air-flow lead crack scenario	87
8.12	Comparison of order tracking results (0% crack to 75% crack) on vertical casing vibration under air-flow lead crack scenario	87
8.13	Comparison of order tracking results (0% crack to 75% crack) on blade vibration under air-flow trail crack scenario.	93
8.14	Comparison of order tracking results (0% crack to 75% crack) on axial casing vibration under air-flow trail crack scenario	94
8.15	Comparison of order tracking results (0% crack to 75% crack) on horizontal casing vibration under air-flow trail crack scenario.	94
8.16	Comparison of order tracking results (0% crack to 75% crack) on vertical casing vibration under air-flow trail crack scenario	94
8.17	Comparison of order tracking results (0% crack to 75% crack) on blade vibration under blade root crack scenario.	101
8.18	Comparison of order tracking results (0% crack to 75% crack) on axial casing vibration under blade root crack scenario	101
8.19	Comparison of order tracking results (0% crack to 75% crack) on horizontal casing vibration under blade root crack scenario	102
8.20	Comparison of order tracking results (0% crack to 75% crack) on vertical casing vibration under blade root crack scenario	102
8.21	Comparison of order tracking results (0% crack to 75% crack) on blade vibration under FOD at blade tip scenario	109
8.22	Comparison of order tracking results(0% crack to 75% crack) on axial casing vibration under FOD at blade tip scenario	109
8.23	Comparison of order tracking results(0% crack to 75% crack) on horizontal casing vibration under FOD at blade tip scenario	110
8.24	Comparison of order tracking results(0% crack to 75% crack) on vertical casing vibration under FOD at blade tip scenario	110
9.1	Correlation between measured data and FEA modeling data	143
9.2	The summary of the consolidated findings.	144

## LIST OF FIGURES

FIGURE NO.	TITLE	PAGE
1.1	Key element for Hot Gas Path Inspection	02
1.2	Mechanism reported to have cause the turbine blade failures ( Dewey & Rieger 1982; Dewey & McClokes 1983; Dewey & Rieger 1983; Artens et al 1984)	03
1.3	Location of LP turbine blade failures (Dewey & Rieger 1982; Dewey & McClokes 1983; Dewey & Rieger 1983; Artens et al 1984)	03
4.1	De-commissioned blades with crack patterns for stationary test condition	17
4.2	Simplified straight blades with crack patterns for dynamic test condition.	17
4.3	Overview of research methodology	18
5.1	Photograph of experimental rig for stationary testing condition	23
5.2	Photograph of an impact hammer with a softtip	24
5.3	Useful range of PCB impact hammer	25
5.4	Comparison of useful range between soft tip and metal tip impact hammer.	25
5.5	IMC Cronos, 8 channels data acquisition system	26
5.6	A miniature accelerometer from Dytran Inc. was used during the stationary and dynamic testing conditions.	26
5.7	Vibration calibrator, VE 10 from RION.	27

5.8	A 4 x 4 array been marked onto the selected blades.	28
5.9	Window to input the instrument parameter during measurement set up	29
5.10	De-commissioned blade in position ready for impact test	29
5.11	Curve fitting function from MeScope	31
6.1	Geometric turbine blade imported from Pro-E to ANSYS.	33
6.2	Material properties for the model	34
6.3	Comparison between normal model (left) to the extreme model (right)	35
6.4	3 DOFs constraints were applied to the model.	36
7.1	Schematic layout of the test rig	39
7.2	Assembly of steel blades to aluminum rotor	40
7.3	Accelerometers setting in dynamic test condition.	41
8.1	Impact test raw time waveform.	45
8.2	Comparison between support responses to an average response	46
8.3	Zoomed in time waveform. No sign of double impacts	46
8.4	Input force decayed from 0 Hz to 10 kHz by using different type of impact hammer's tip.	47
8.5	FRFs for 16 measurement points under 1 scenario	48
8.6	Mescope -curve fitting function.	49
8.7	Blade with Airflow lead crack (75% crack of platform length-3 <sup>rd</sup> cut)	50
8.8	Global mode animation v.s. local mode animations; global mode move homogenously, while local modes move individually	51
8.9	Comparison of 1st and 2nd modes' mode shape; different movement yields different impact from the crack type and length	52
8.10	Air-flow Lead Crack: Changes of natural frequencies to different crack length	52
8.11	Blade with Airflow trail crack (75% crack of platform length-3 <sup>rd</sup> cut)	54
8.12	Air-flow Trail Crack: Changes of natural frequencies to different crack length	55

8.13	Animation of 5 <sup>th</sup> mode under airflow trail crack after the 3rd cut, 75% crack of platform length.	56
8.14	Blade with root crack (75% crack of platform length-3rd cut)	57
8.15	The animation of 10th mode under blade root crack, where all most all movement concentrated at blade tip.	58
8.16	Blade Root Crack: Changes of natural frequencies to different crack	85
8.17	Blade with FOD at blade tip	60
8.18	Homogenous movement of lower modes (3rd & 4th mode)	61
8.19	FOD at Blade Tip: Changes of natural frequencies to different crack length	61
8.20	Comparison between normal condition and extreme case	63
8.21	Homogenous movement (1st mode) vs. localize movement (5th mode) in ANSYS modeling	63
8.22	Turbine Blade FEA modeling under airflow lead crack	65
8.23	FEA: Air-flow Lead Crack: Changes of natural frequencies to difference crack length	65
8.24	Turbine Blade FEA modeling under airflow trail crack	67
8.25	FEA: Air-flow Trail Crack: Changes of natural frequencies to different crack length	67
8.26	Turbine Blade FEA modeling under blade root crack	69
8.27	FEA: Root Blade Crack: Changes of natural frequencies to different crack length	69
8.28	Turbine Blade FEA modeling under FOD.	71
8.29	FEA: FOD at Blade Tip: Changes of natural frequencies to different crack length	71
8.30	Repeatability test results for dynamic test condition; run up measurements at casing; axial, horizontal and vertical directions.	73

8.31	Repeatability test results for dynamic test condition; steady state measurements at casing; axial, horizontal and vertical directions.	73
8.32	TWF of blade compare to TWF of tachometer in a baseline complete cycle.	74
8.33	Zoomed in: TWF of blade compare to TWF of tachometer in a complete cycle of baseline measurement	75
8.34	TWF of tri-axis compare to TWF tachometer in a complete cycle of baseline measurement	75
8.35	Zoomed in: TWF of tri-axis compare to tachometer TWF in a complete cycle of baseline measurement	76
8.36	Color map of blade vibration under air-flow lead crack pattern. Comparison of 0% to 75% crack length.	78
8.37	The 4th order of run up and coast down results (acceleration) for blade vibration under air-flow lead crack pattern.	79
8.38	The 4th order of run up and coast down results (velocity) for blade vibration under air-flow lead crack pattern.	79
8.39	The 5th order of run up and coast down results (acceleration) for blade vibration under air-flow lead crack pattern.	80
8.40	The 5th order of run up and coast down results (velocity) for blade vibration under air-flow lead crack pattern.	80
8.41	Color map of axial casing vibration under air-flow lead cracked. Comparison of 0% to 75% crack length.	82
8.42	Color map of horizontal casing vibration under air-flow lead cracked. Comparison of 0% to 75% crack length	83
8.43	Color map of vertical casing vibration under air-flow lead cracked. Comparison of 0% to 75% crack length	84
8.44	The 10th order of run up and coast down results (acceleration) for axial casing vibration under air-flow lead crack pattern	85
8.45	The 12th order of run up and coast down results (acceleration) for axial casing vibration under air-flow lead crack pattern.	85
8.46	The 12th order of run up and coast down results (acceleration) for horizontal casing vibration under air-flow lead crack pattern.	86



8.47	The 12th order of run up and coast down results (acceleration) for vertical casing vibration under air-flow lead crack pattern.	86
8.48	Coast down wavelet map of blade vibration under air-flow lead crack pattern	89
8.49	Coast down wavelet map of axial casing vibration under air-flow lead crack pattern	90
8.50	Coast down wavelet map of horizontal casing vibration under air-flow lead crack pattern	91
8.51	Coast down wavelet map of vertical casing vibration under air-flow lead crack pattern	92
8.52	The 5th order of coast down results (acceleration) for blade vibration under air-flow trail crack pattern	95
8.52	The 12th order of coast down results (acceleration) for axial casing vibration under air-flow trail crack pattern.	95
8.54	The 12th order of coast down results (acceleration) for horizontal casing vibration under air-flow trail crack pattern	96
8.55	The 12th order of coast down results (acceleration) for vertical casing vibration under air-flow trail crack pattern.	96
8.56	Coast down wavelet map of blade vibration under air-flow trail crack pattern	97
8.57	Coast down wavelet map of axial casing vibration under air-flow trail crack pattern	98
8.58	Coast down wavelet map of horizontal casing vibration under air-flow trail crack pattern	99
8.59	Coast down wavelet map of vertical casing vibration under air-flow trail crack pattern	100
8.60	The 1st order of coast down results (acceleration) for blade vibration under blade root crack pattern	103
8.61	The 12th order of coast down results (acceleration) for axial casing vibration under blade root crack pattern.	103
8.62	The 12th order of coast down results (acceleration) for horizontal casing vibration under blade root crack pattern	104
8.63	The 12th order of coast down results (acceleration) for vertical casing vibration under blade root crack pattern.	104

8.64	Coast down wavelet map of blade vibration under blade root crack pattern	105
8.65	Coast down wavelet map of axial casing vibration under blade root crack pattern	116
8.66	Coast down wavelet map of horizontal casing vibration under blade root crack pattern	107
8.67	Coast down wavelet map of vertical casing vibration under blade root crack pattern	108
8.68	The 1st order of coast down results (acceleration) for blade vibration under FOD a blade tip.	111
8.69	The 1st & 12th order coast down results (acceleration) for axial casing vibration under air-flow lead crack pattern.	111
8.70	The 1st & 12th order coast down results (acceleration) for horizontal casing vibration under air-flow lead crack pattern	112
8.71	The 1st & 12th order coast down results (acceleration) for vertical casing vibration under air-flow lead crack pattern	112
8.72	Coast down wavelet map of blade vibration under FOD at blade tip.	113
8.73	Coast down wavelet map of axial casing vibration under FOD at blade tip.	114
8.74	Coast down wavelet map of horizontal casing vibration under FOD at blade tip.	115
8.75	Coast down wavelet map of vertical casing vibration under FOD at blade tip.	116
8.76	‘Cleaner’ spectrum from PDS(below) compared to conventional FFT(above)	117
8.77	The PDS in velocity (blow) is more sensitive to capture the low frequency changes.	117
8.78	The steady state PDS (velocity) of blade vibration under air-flow lead crack pattern.	118
8.79	The steady state PDS (velocity) of axial casing vibration under air-flow lead crack pattern.	119
8.80	The steady state PDS (velocity) of horizontal casing vibration under air-flow lead crack pattern.	119

8.81	The steady state PDS (velocity) of vertical casing vibration under air-flow lead crack pattern.	120
8.82	Steady state wavelet map of blade vibration under air-flow lead crack pattern	121
8.83	Steady state wavelet map of axial casing vibration under air-flow lead crack pattern	122
8.84	Steady state wavelet map of horizontal casing vibration under air-flow lead crack pattern	123
8.85	Steady state wavelet map of vertical casing vibration under air-flow lead crack pattern	124
8.86	The steady state PDS (velocity) of blade vibration under air-flow trail crack pattern.	125
8.87	The steady state PDS (velocity) of axial casing vibration under air-flow trail crack pattern	125
8.88	The steady state PDS (velocity) of horizontal casing vibration under air-flow trail crack pattern	126
8.89	The steady state PDS (velocity) of vertical casing vibration under air-flow trail crack pattern	126
8.90	The steady state PDS (velocity) of blade vibration under blade root crack pattern	127
8.91	The steady state PDS (velocity) of axial casing vibration under blade root crack pattern	128
8.92	The steady state PDS (velocity) of horizontal casing vibration under blade root crack pattern	128
8.93	The steady state PDS (velocity) of vertical casing vibration under blade root crack pattern	129
8.94	The steady state PDS (velocity) of blade vibration under FOD at blade tip crack pattern	130
8.95	The steady state PDS (velocity) of axial casing vibration under FOD at blade tip crack pattern	130
8.96	The steady state PDS (velocity) of horizontal casing vibration under FOD at blade tip crack pattern	131

8.97	The steady state PDS (velocity) of vertical casing vibration under FOD at blade tip crack pattern	131
9.1	Validation of FEA model to the measured data under air-flow lead crack pattern.	133
9.2	Validation of FEA model to the measured data under air-flow trail crack pattern	134
9.3	Validation of FEA model to the measured data under blade root crack pattern	134
9.4	Validation of FEA model to the measured data under FOD at blade tip crack pattern	135
9.5	Made shape comparison of measured data (above) to FEA model (below), 0% crack @ 1st mode.	136
9.6	Made shape comparison of measured data (above) to FEA model (below), 0% crack @ 2nd mode.	137
9.7	Made shape comparison of measured data (above) to FEA model (below), 0% crack @ 3rd mode.	138
9.8	Made shape comparison of measured data (above) to FEA model (below), 0% crack @ 4th mode.	139
9.9	The 5th order of coast down results (acceleration) for blade vibration under blade root crack pattern	141

**LIST OF ABBREVIATIONS**

BPS	-	Blade Passing Frequency
CWT	-	Continuous Wavelet Transform
Hz	-	Hertz
FFT	-	Fast Fourier Transform
FOD	-	Foreign Object Damage
FRF	-	Frequency Response Function
PDS	-	Power Density Spectrum
RPM	-	Revolution per minute
STFT	-	Short Time Fourier Transform

**LIST OF APPENDICES**

<b>APPENDIX</b>	<b>TITLE</b>	<b>PAGE</b>
A1	Wavelet Analysis	153
A2	Order Tracking	163
A3	Power Density Spectrum	171
A4	Accelerometer Catalogs	177

## CHAPTER 1

### INTRODUCTION

#### 1.1 Overview

Gas turbines are common but critical machines used in power generation, petrochemical and heavy industries. Unscheduled down time often result in economic losses exceeding RM1million per day [1]. With such economic losses quick diagnosis and trouble shooting is required. [2] Manufactures such as General Electric [3], recommends 3 types of maintenance inspections namely standby, running and disassembly inspections to prevent unscheduled down time. Turbine blades being key components of the gas turbine which suffers high mechanical loading due to drastic changes in both temperature and pressure. [4] These often result in mechanical failures such as cracking, blade rubbing, degradation etc which are often detected only during the Hot Gas Path Inspection under the disassembly inspection [3]. Figure 1.1 provided an overview of the work scope during the inspection. Minor repair could be carried at the same time. Tim J Carter (2004) reported that turbine blade suffered most damage from crack which were either caused by foreign object damage (FOD) or torsional forces. This is illustrated in the figure 1.2. This figure shows possible turbine blade failures and the percentage distribution. Cracks on surface, like which occurs on aerofoil & lashing area are not as harmful as compared those in the blade root and disk root area; as long the failure

does not penetrate through the blade body. These are also relatively easier to be detected during the visual inspection by applying the Fluorescent Penetrate Inspection (FPI) or non- Destructive Inspection (NDI) [3]. Cracks adjacent the blade clamp area are potentially very serious as it is not so visual and are difficult to detect unless during the Major Inspection [3] where all turbine blades would be removed from the rotor. The percentage of blade root cracking is also significant. This is illustrated in figure 1.3. It had been reported that cracks in the air-flow lead and trailing edge also recorded high percentage. Normally the stress rupture crack will appear in these areas. The latter experiments would be based on these crack patterns.

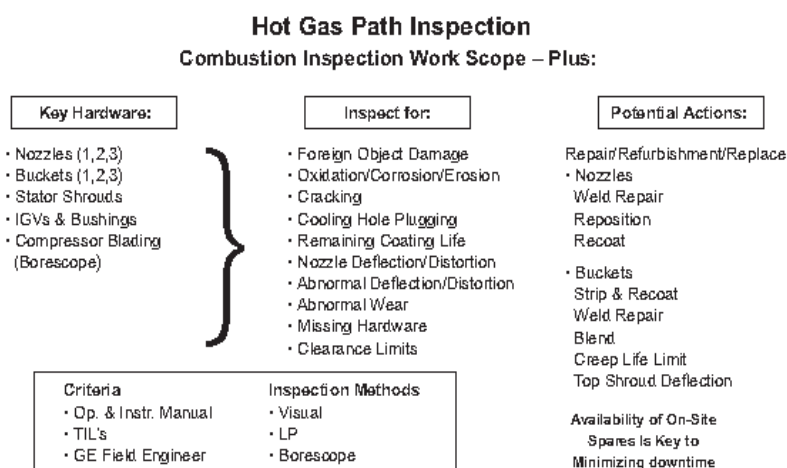


**Figure 1.1** Key element for Hot Gas Path Inspection



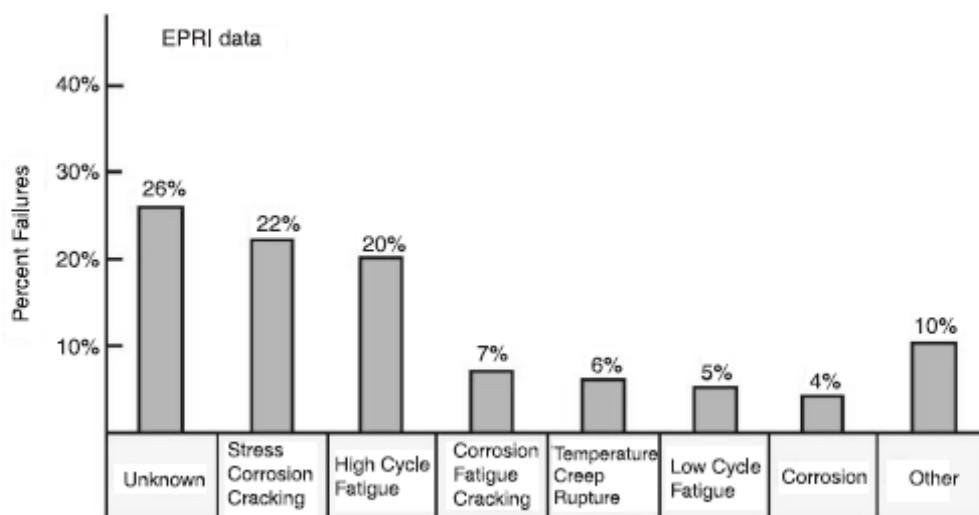


**Figure 1.2** Mechanism reported to have caused the turbine blade failures (Dewey & Rieger 1982; Dewey & McClokes 1983; Dewey & Rieger 1983; Artens *et al* 1984)

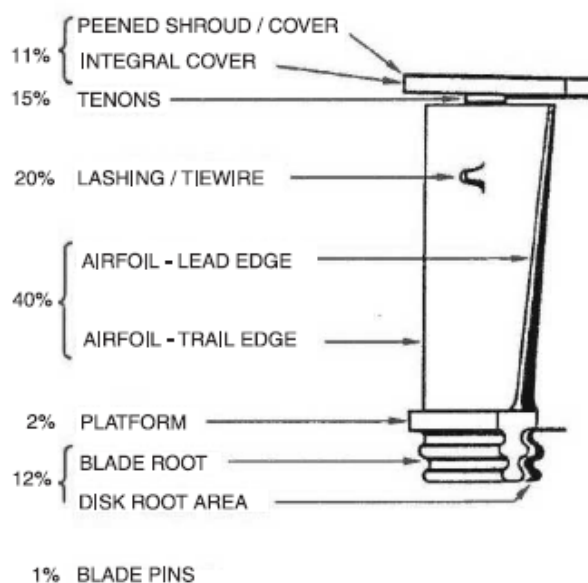


**Figure 1.3** Location of LP turbine blade failures (Dewey & Rieger 1982; Dewey & McClokes 1983; Dewey & Rieger 1983; Artens *et al* 1984)

## 1.2 Subject Background

A gas turbine is a complicated machine. A turbine blade has to withstand the vibratory stresses, flexural stresses, centrifugal force etc. Basically the vibratory stresses are induced by aerodynamic forces. These forces are introduced by the combusted gas that flow through the stages of blades. Centrifugal forces are the side effects of the gas turbine rotational movement. Increase of the rotational speed would double up the forces value; therefore proper blade design is very important. The flexural stresses are generated by the motion of the blade that causes an unsteady pressure field around the blade sustaining the vibration. This excitation is initiated by small mechanical or aerodynamic disturbances above the critical flow speed.

Turbine blade life cycle is influenced by factors which under two main categories: design and operation conditions; Operation condition are more critical category. Blades have to maintain its integrity under severe operation conditions which result in high mechanical stress and high thermal stresses [5].

Turbine blades operate at high temperatures, typically up to 1000<sup>0</sup>C. At the same time blades are exposed to contamination issue mainly from burning fuel and intake air. Foreign object damage (FOD) is a common occurrence where blades are damages with material removed from impurities and foreign objects impinging on the blades.

Thermal stresses occur in the blade when the blade is experiencing the large scale thermal gradient. This often happen during the transient states like run up or coast down. This stress normally concentrated to the tip or edges or of the blade which results in crack on the blade.

Blade vibrations are often examined under two different perspectives: self excited vibration and forced vibration. Self excited vibration is often known as flutter. It is an aero-elastic self-induced vibration with a sustained amplitude, normally seen at high speed rotation with no external forces involved. Force vibration is induced by flow disturbances when working fluids pass through the stages. This would results in an impulsive force to the blade body.

Blade vibration could only be measured from the casing and under such situation would not off any direct measurement of the blade induced vibration. Even though the blade vibration could not be measured directly, blade related diagnosis still could be done from examination of response related to blade pass frequencies (BPF).

The BPF is the pulsation force which occurs in bladed assembly. This force is generated from the pressure fluctuation as a rotating vane or blade passes stationary components like stator or housing. The stationary component produces a non-uniform flow disturbance in the gas field. In vibration analysis, the number of blades multiplied with the RPM of the rotor supporting the impeller physically defines the blade passing frequency (BPF). The amplitude corresponding to the BPF is small. An increase in the vibration amplitude of the BFP is usually due to:

- (i ) A housing or rotor eccentricity
- (ii ) Vane or blade wear (abrasive materials)
- (iii) Bent, loose or misaligned housing diffuser vane
- (iv ) A resonance Excitation

### 1.3 Problem Statement

The manufacture's Major Inspection undertaken for gas turbine is expensive and requires a long downtime. It is usually scheduled according to the manufacturer's recommendations or based on findings of previous inspection results. This is normally undertaken 2-3 years after the turbine's initial operation. With thermal stresses from periodic on-off, turbine blade cracks had known to occur rapidly with serious consequences prior to the Major Inspection. [6]

It is then very important to indicate the present of cracked blade from the non-invasive measurements or procedures such as vibration. The current operational vibration monitoring which mainly focus on overall vibration value, showed insufficient sensitivity in detecting the cracked blade. Vibration FFT plots obtained under steady state condition are also not sensitive enough for the detection of cracked blade. Sophisticated analysis method such as order tracking, power density spectrum and wavelet analysis could be considered to be used in maintenance inspection especially it shown to be able to detect crack blade.

The visual inspection undertaken during maintenance relies on visual means and human interpretation. Minute cracks or blade root crack could be missed out easily during the visual inspection. A scientific based method such as the impact test could be used as a more reliable tool to assist the visual inspection during maintenance.

An understanding of dynamic behavior of a cracked blade needs to be obtained prior to application in the maintenance inspection.

#### **1.4 Objectives of the study**

The objective of this study was to assess the practicability of vibration based test method in detecting cracks in turbine blade. This can be explained as follow,

1. To verify the effectiveness of vibration impact test to capture the turbine blade crack in a minor inspection. This required the study cracked blade response from the impact tests.
2. To model a blade with or without cracks using FEA method. Computational results would be correlated against the measurement results.
3. To study which vibration analysis methods (order tracking, FFT and wavelet) for a rotating blade assembly for the detection of a cracked blade from the measured vibration response.

#### **1.5 Scopes of the study**

The scope of this research were limited to the followings,

1. The identification of a common crack patterns that occur in real blades.
2. An experimental study for vibration response of stationary blades from impact test for blades with the common crack patterns..
3. The comprehension of cracked blade effects from computational model and modal analysis.
4. An experimental study of vibration measurement analysis for a rotating bladed assembly with induced cracks in a test rig.